Bollettino di Geofisica Teorica ed Applicata Vol. 53, n. 1, pp. 55-74; March 2012
DOI 10.4430/bgta0040

Quantifying probabilities of eruption at a well-monitored active volcano: an application to Mt. Etna (Sicily, Italy)

A. Brancato[1], S. Gresta[1], L. Sandri[2], J. Selva[2], W. Marzocchi[3], S. Alparone[4], D. Andronico[4], A. Bonforte[4], T. Caltabiano[4], O. Cocina[4], R.A. Corsaro[4], R. Cristofolini[1], G. Di Grazia[4], G. Distefano[1], C. Ferlito[1], S. Gambino[4], S. Giammanco[4], F. Greco[4], R. Napoli[4], G. Tusa[1] and M. Viccaro[1]

[1] *Dipartimento di Scienze Geologiche, University of Catania, Italy*
[2] *INGV – Sezione di Bologna, Italy*
[3] *INGV – Sezione di Roma, Italy*
[4] *INGV – Sezione di Catania, Italy*

(Received: April 30, 2010; accepted: November 17, 2010)

ABSTRACT At active volcanoes, distinct eruptions are preceded by complex and different precursory patterns; in addition, there are precursory signals that do not necessarily lead to an eruption. The main purpose of this paper is to present an unprecedented application of the recently developed code named BET_EF (Bayesian Event Tree_Eruption Forecasting) to the quantitative estimate of the eruptive hazard at Mt. Etna volcano. We tested the model for the case history of the July-August 2001 flank eruption. Anomalies in geophysical, geochemical and volcanological monitoring parameters were observed more than a month in advance of the effective onset of the eruption. As a consequence, eruption probabilities larger than 90% were estimated. An important feature of the application of BET_EF to Mt. Etna was the probabilistic estimate of opening vent locations. The methodology allowed a clear identification of assumptions and the monitoring of parameter thresholds and provided rational means for their revision if new data or information are incoming.

Key words: Mt. Etna, eruption forecasting, Bayesian event tree.

1. Introduction

The evaluation of volcanic hazard (i.e., the probability that a specific area will be affected by eruptive phenomena within a given time period) is mainly based on the past behaviour of the volcano under study and on topographical parameters. Under the assumption that the character of future events will most likely be similar to some of the past eruptions, the evaluation of volcanic hazard requires an accurate knowledge of past events, mainly based on the historical records coupled with the modern monitoring surveillance procedures. A further important issue is to understand the dynamics of the studied volcano, such as its tectonic and geological environment, the magma supply into reservoirs below or within the volcanic edifice, the processes of magma reaching the surface, as well as the detailed knowledge of the monitoring time series preceding the eruption events. The frequency and character of eruptions are largely under the control of these factors.

Mt. Etna is a basaltic stratovolcano with persistent volcanic activity. The volcano is located

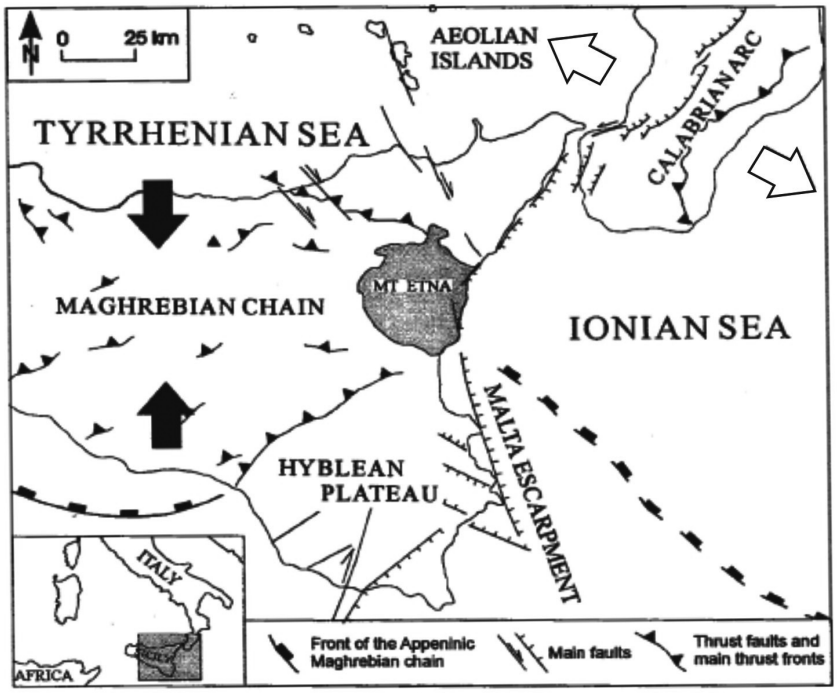

Fig. 1 - Main regional tectonic features of the Mt. Etna area. Black arrows indicate the compressive domain of western-central Sicily, related to the Africa-Europe collision; white arrows indicate the extensional domain of the Calabrian Arc (after Cocina *et al*., 1998).

along the eastern coast of Sicily, between the compressive domain of western-central Sicily and the extensional domain of the Calabrian Arc (Fig. 1), being the most active volcano in the Mediterranean area (about 3350 m a.s.l.), and one of the best monitored worldwide (Bonaccorso *et al*., 2004a). Volcanic activity (Fig. 2) ranges from quasi-continuous summit to quite frequent flank eruptions (Guest, 1982; Cristofolini *et al*., 1988; Branca and Del Carlo, 2005). Apart from the rare sub-Plinian explosive eruptions, summit activity is mostly characterized by continuous degassing, Strombolian ejections, lava fountaining and small lava effusions. On the contrary, flank eruptions take place at intervals of years, producing lava effusion commonly associated with explosive activity (either at summit craters or at flank vents). These eruptions originate from fractures that open on the flanks of the volcano, giving origin to lava fields of several square kilometres, and with durations spanning from days to years.

Apart from an almost continuous activity at the summit craters, the July-August 2001 eruption represents the re-start of the flank activity after the December 1991-March 1993 large flank eruption. During the 1993-2000 time period, the volcano monitoring was deeply improved with a technical and numerical upgrading of the pre-existent operating networks (seismic, ground deformation, gravimetric and geochemistry fluids) and with the installation of a magnetic network. Therefore, the July-August 2001 represents the first history case of a flank eruption at Mt. Etna monitored through these innovative supplements.

Moreover, this eruption was characterised by an unusual eruptive style, with both lava-flow emissions from different fractures and powerful Strombolian activity, sometimes yielding to lava fountaining episodes. In addition, the eruption was shortly preceded by one of the most intense seismic swarms of the last 20 years (Patanè *et al*., 2003). A seismic swarm of more than 2,600

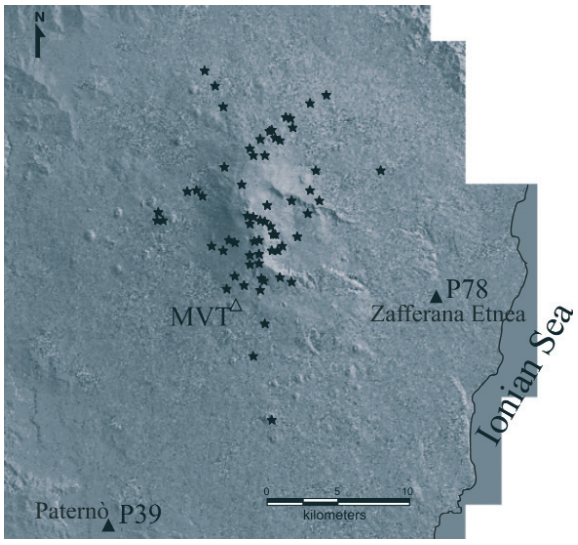

Fig. 2 - Sketch map of Mt. Etna. Also shown the location of the vents (black stars) of the flank eruptions that occurred at Mt. Etna over the 20th century, P39 and P78 gas sites sampling (filled triangles), and the MVT seismic station (open triangle), whose records are used in this study. The thin, black line borders the eastern coast of Sicily.

events in less than 4 days gave evidence that a dyke was emplaced on July 12 (Patanè *et al*., 2003), as confirmed by GPS and tilt data (Bonaccorso *et al*. 2002). By July, a system of dry fissures striking N-S opened south of the still erupting south-eastern crater (hereafter, SEC); whereas the eruption started on July 17. Three main eruptive vents and some further minor eruptive fractures opened at altitudes between 2100 m and 3000 m a.s.l. At least two different uprising magma paths have been defined (Monaco *et al*., 2005). The whole southern flank of the volcano was involved in the eruption (Fig. 3). The rate of lava emission suddenly dropped on July 31 and on August 9, the eruption stopped completely (Falsaperla *et al*., 2005).

The aim of this paper is a retrospective analysis of the estimation of the eruption probability at Mt. Etna during the time period January-July 2001, by using an event tree probability [BET_EF: i.e., Marzocchi *et al*. (2004, 2008)]. This provides multiple possible outcomes. The first step of the work will be the "elicitation" of the parameters for the different nodes of the tree. Then, anomalies in geophysical, geochemical and volcanological monitoring parameters will be taken into account, providing the probabilistic estimate of the flank eruption occurrence, as well as of the rough location of the eruptive vents.

2. BET_EF (Bayesian Event Tree for Eruption Forecasting) code (version 2.1)

The BET_EF algorithm is a code implementing a Bayesian Event Tree to compute the probabilities of specific volcanic events of interest (e.g., an eruption, an eruptive vent location, an eruption of a specific size/style) by merging all relevant, available information retrieved by theoretical models, a priori beliefs, monitoring measurements, expert opinions, and past data (i.e., all the information deriving from stratigraphy, geology, historic records, etc.).

The BET_EF model, based on the event tree philosophy proposed by Newhall and Hoblitt (2002), further develops the concepts of vent location, epistemic and aleatory uncertainties (respectively associated with the lack of knowledge of the processes involved in a

volcanic system, and with the intrinsic unpredictability of the phenomena), and a fuzzy approach for monitoring measurements in order to simulate the expert opinion with a given anomaly degree of the observed parameters. The method is discussed in Marzocchi *et al*. (2008), and we refer the reader to this paper for all the details. Here, we only remind you that the code is based on an event tree, where individual branches are alternative steps from a general prior event, and evolve into increasingly specific subsequent states (Fig. 4a). The points on the graph where new branches are set are referred to as *nodes* (Newhall and Hoblitt, 2002; Marzocchi *et al*., 2004, 2008); in detail:

Node 1: it is related to the probability of having an unrest over the time interval $[t_0, t_0 + \tau]$, where t_0 is the present time, and τ is the time window considered;

Node 2: the unrest has a magmatic origin or is related to other causes (e.g., hydrothermal or tectonic activity), providing that an unrest has been detected;

Node 3: the magma will or will not erupt over the time interval $[t_0, t_0 + \tau]$, providing that the unrest has a magmatic origin;

Node 4: the vent will open at a specific location, provided that there is an eruption;

Node 5: the eruption will be of a given size/style, provided that an eruption occurs at a specific vent.

In the BET_EF model, the forecast window time τ, to which the probability estimates are referred, is not fixed a priori, but is set by the user on the grounds of the observed typical time scale of variations in the state of the volcano under study. For example, if the considered volcano shows variations of its state typically with long-term behaviour (years), then mid-term probability estimates (e.g., a month) will be suitable. This application has been theoretically tested for long-time quiescent volcanoes [e.g., Vesuvius, see Marzocchi *et al*. (2004, 2008); Campi Flegrei, see Orsi *et al*. (2009); Auckland Volcanic Field, see Lindsay *et al*. (2010)].

The BET_EF gives quantitative probability estimates of specific eruption-related outcomes through the evaluation of the probability density functions of the above five nodes by merging past data and models, and monitoring information. Generally speaking, the code (Marzocchi *et al*., 2004, 2008) consists of a *non monitoring* and *monitoring* components, computed through Bayesian inference (Fig. 4b). Regarding the non-monitoring component, the a priori distribution at each node describes a general knowledge about that specific node (e.g., expert opinion and/or experiences gained from similar volcanic activity worldwide), represented by a 'best guess' probability and a weight associated to such guess, expressed as 'equivalent number of data' (Λ). A guess with a low Λ has a very low reliability; in contrast, when there is a significant convergence of the expert opinions on the best guess provided, Λ will be high. For further details, see Marzocchi *et al*. (2004, 2008).

The likelihood function of the non-monitoring section is shaped on the grounds of past data. If the number of past data is larger than the 'equivalent number of data', it yields to a larger influence on the final a posteriori distribution. On the contrary, if the number of past data is comparable to the 'equivalent number of data', the a posteriori distribution will be the result of a weighted merging of both components.

The a priori distribution of the monitoring component is derived by using parameters usually managed and measured during volcano surveillance activities. These parameters can be chosen by experts, along with their lower and upper thresholds in a fuzzy perspective, used to relate a given anomaly degree in order to simulate the expert judgement (Marzocchi *et al*., 2008). At

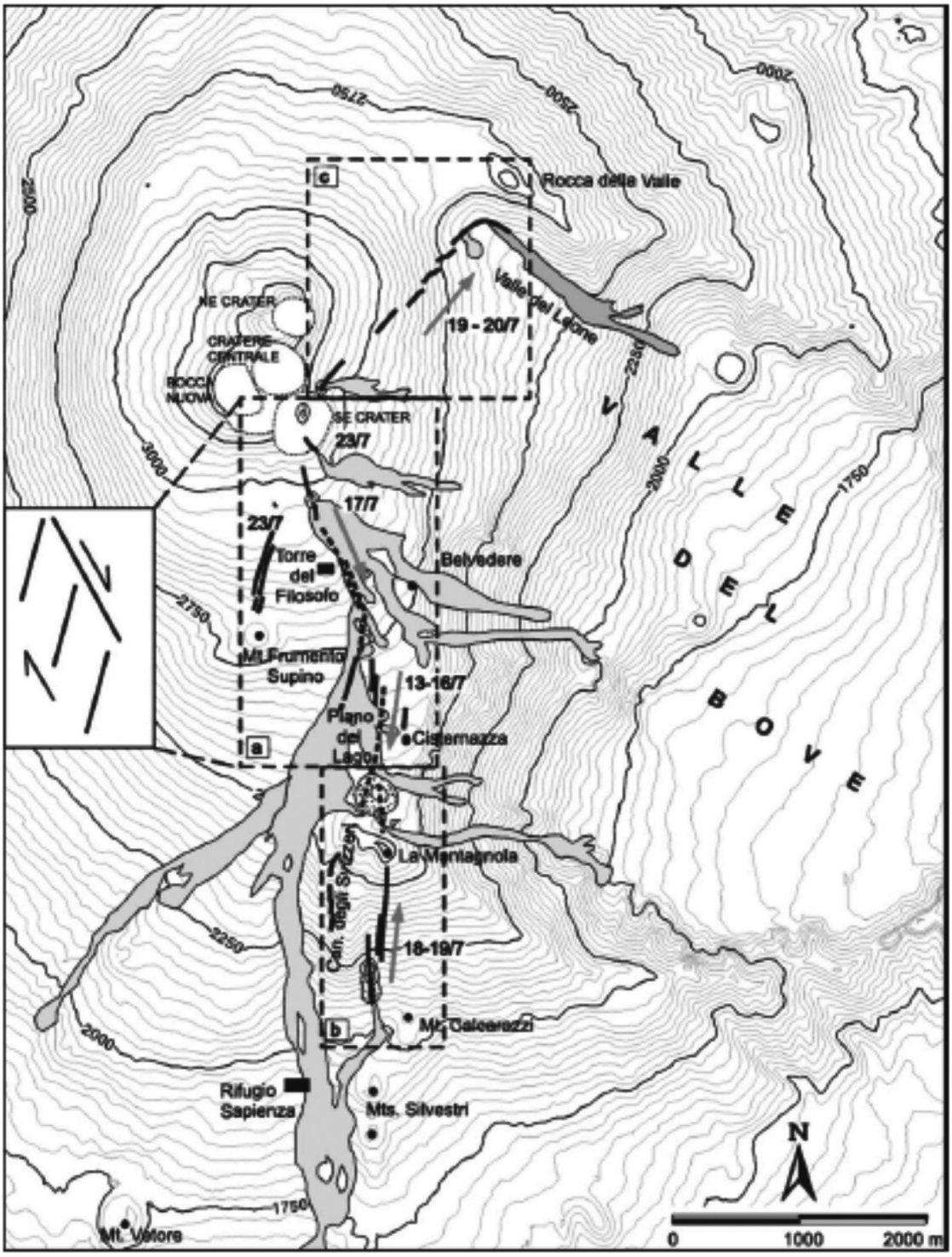

Fig. 3 - Map of the eruptive fracture systems and lava flows formed during the 2001 July 17-August 9 flank eruption. Three main fracture fields have been recognized on the basis of the time–space development of distinct segments: (a) Piano del Lago field; (b) Montagnola field; (c) Valle del Leone field. Gray arrows indicate the sense of migration of each fracture field (after Monaco *et al*., 2005).

nodes 2 and 3, the BET_EF needs to assign a weight to each monitored chosen parameter. This is because the code recognizes the capacity of some monitoring measurements (e.g., earthquakes occurring, tremor and gravity data) to indicate much better than others the evolution of the state of the volcano. A weight equal to 2, implies that the parameter is a strong indicator for the relative node, and, for example, an anomalous parameter with weight 2 is the equivalent of two anomalous parameters with weight equal to 1. The a priori distribution is then adapted by the likelihood function if past data from actual monitored unrest or eruptive events are available.

3. Setting up BET_EF for Mt. Etna

In general, any model and input data used to set up the code are selected by following the basic principles of simplicity and acceptance by a wide scientific community. In practice, the starting point is always assumed as a state of maximum ignorance (i.e., no possibility is excluded). Probability estimates are then revised (in a Bayesian framework) based on the availability of robust and widely accepted models and data.

First of all, it is necessary to define a suitable time window for the BET_EF forecast. It must be shorter than, or comparable to, the typical time scale of the variations in the state of the volcano. As Mt. Etna is an open-conduit persistently active volcano, significant variations of the monitored parameters are expected to occur over time scales of hours (mainly for the activity at the summit craters) to days or weeks (for flank eruptions). In this case, the most suitable forecast time window will be necessarily short; therefore, we fixed $\tau = 1$ week.

For short-term eruption forecasting, the monitoring has a leading role, primarily based on seismological data and volcanological observations, integrated with strain, fluid geochemistry, gravimetric and magnetic data. As a consequence, relevant parameters and relative thresholds were fixed before any run of the code during several expert elicitation sessions. The criteria of such a selection are based on what is the present surveillance system on Mt. Etna. Nevertheless a magnetic network has been deployed in the last decade, relative data is not included in the present running because of some incoherency in node 3. Therefore, in the case of the 2001 eruptive activity forecast, we collected 39 monitoring parameters, distinct for nodes and activity.

The "inertia" problem was also discussed and fixed. We used a boxcar shaped inertia time window. As a consequence, the contribution of any anomalous parameter to the definition of node probabilities will completely vanish after expiration of the inertia time. For example, at node 1, for the parameter "Number of Volcanic-Tectonic (hereafter, VT) earthquakes (M=1+)", a 6-month inertia means that, according to the experts, a daily VT number > 5 opens a 6 months window for the duration of the unrest activity. The parameter is slightly changed in nodes 2 and 3 ["Number of VT earthquakes (D<5 km)"] with different thresholds (>3 and >40 events per day, respectively), with different inertia times, although shorter in these nodes (3 months and 1 day, respectively). In Table 1, we report all the setting (monitoring parameters, and relative thresholds and "inertia" time periods), node by node, for the application of the BET_EF to Mt. Etna.

In the following, we give some brief explanation of the choices made at each node.

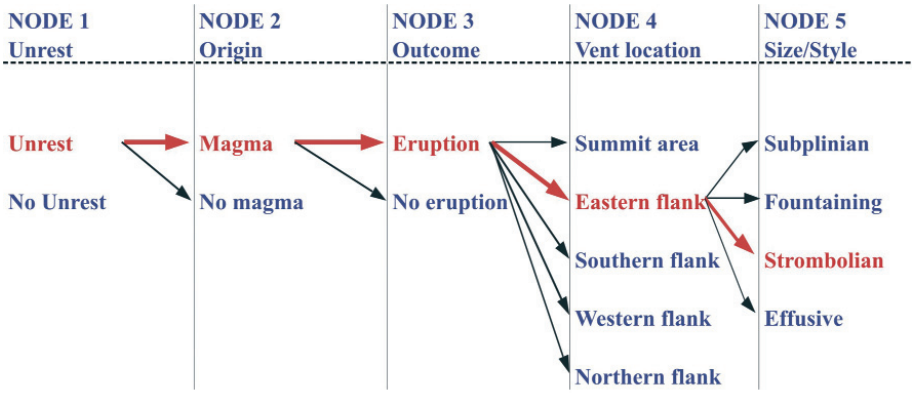

a.

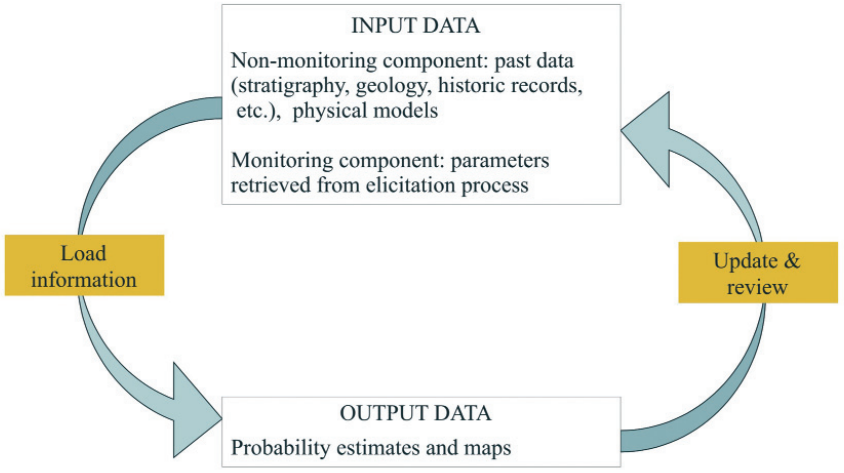

b.

Fig. 4 - General scheme of the BET_EF code (selection of the path, within the event tree) as adapted for the present application (a.), and simplified flow-chart of the run process (b.).

3.1. Node 1: unrest / no unrest

3.1.1. Non-monitoring component

A priori distribution. No information is available; then, a uniform distribution (representing maximum ignorance, see above) is assumed.

Past data. We retrieved information from a seismic catalogue of recorded events at the MVT station (see Fig. 2) during the period January 1980 – December 1990, our aim being a retrospective application of BET_EF starting from 1991. In this time interval, 17 eruptions were reported by Branca and Del Carlo (2005). Therefore, we needed to count the number of unrest episodes (eruptive or not). Non-eruptive unrest episodes were roughly defined by looking at the average daily rate of earthquakes recorded at the MVT station. Since, on average, there are 3 events per day, we defined an unrest episode when a conservative number of 35 earthquakes per week were recorded at the MVT station. Based on this broad definition, we counted 14 unrest

Table 1 - Summary of the BET_EF input information (prior models, past data and monitoring parameters) for the 2001 July-August eruption at Mt. Etna. Also shown thresholds and inertia of the collected parameters. In third column, the superscript a stands for the weight of the monitoring parameter, as well the superscript b represents the number of the equivalent data for non-monitoring components.

Input Parameter	Data/Thresholds/Inertia	W^a/Λ^b
NODE 1: Unrest/No Unrest		
Prior distribution	No info (uniform distribution)	
Past data	n_1=329 weeks; y_1=31	
Number of earthquakes (D≥200 km; M=5+; Tyrrhenian slab)	>1 day^{-1}; 3 months	
Number of VT earthquakes (M=3+; Pernicana Fault)	>1 day^{-1}; 2 months	
Number of VT earthquakes (D≥20 km; M=3+; NW sector)	>1, 3 month^{-1}; 5 months	
Number of VT earthquakes (M=1+)	>5 day^{-1}; 6 months	
Tremor amplitude duplication in 24 h	=1; 1 month	
W flank dilatation	>0.010; 0.015 μstrain day^{-1}; 1 year	
Serra Pizzuta – M. Stempato line	>0.030; 0.055 μstrain day^{-1}; 6 months	
M. Siilvestri – Bocche 1792 line	>0.030; 0.080 μstrain day^{-1}; 6 months	
EDM	>0.070; 0.095 μstrain day^{-1}; 1 year	
Deformation Pernicana Fault	>0.008; 0.020 cm day^{-1}; 3 months	
Clinometric variation (>0.033 μrad day^{-1} ; CDV station)	=1; 1 year	
SO_2 emission	<1500 ton day^{-1}; 3 months	
CO_2 emission (P39 station)	<200 g m^{-2} day^{-1}; 1 week	
Gravity (E-W profile)	>0.35; 0.50 μGal day^{-1}; 2 months	
Gravity (N-S profile; seasonal)	>0.50; 0.70 μGal day^{-1}; 2 months	
Ash emission	=1; 3 months	
NODE 2: Magma/No Magma		
Prior distribution	0.95	1^b
Past data	No data	
Number of VT earthquakes (M=2+; W sector)	>10, 15 day^{-1}; 3 months	2^a
Number of VT earthquakes (D<5 km)	>3 day^{-1}; 3 months	2^a
Number of seismic swarms (>30 earthquakes day^{-1})	=1; 2 months	2^a
W flank dilatation	>0.010, 0.015 μstrain day^{-1}; 1 year	1^a
Serra Pizzuta – M. Stempato line	>0.055, 0.550 μstrain day^{-1}; 6 months	1^a
M. Silvestri – Bocche 1792 line	>0.080, 0.550 μstrain day^{-1}; 6 months	1^a
Clinometric Variation (>1 μrad hour-^{1}; 3 stations)	=1; 0	1^a
SO_2 Emission (variation of >2000 ton day^{-1})	=1; 1 month	1^a
CO_2 emission (P78 station)	<100 g m-^{2} day^{-1}; 2 days	1^a
Gravity (E-W profile)	>0.50, 1.00 μGal day^{-1}; 1 month	1^a
Gravity (N-S profile; seasonal)	>0.70, 1.35 μGal day^{-1}; 1 month	1^a
Juvenile material	=1; 3 months	1^a

Table 1 - Continued.

Input Parameter	Data/Thresholds/Inertia	W^a/Λ^b
NODE 3: Eruption/No Eruption		
Prior distribution	No info (uniform distribution)	
Past data	n_3=31; y_3=17	
Number of VT earthquakes (D<5km)	>40 day^{-1}; 1 day	2^a
Number of VT events	>100 day^{-1}; 1 day	2^a
Tremor (STA/LTA maximum peak)	>2, 4 day^{-1}; 1 day	2^a
W flank dilatation	>0.025, 0.025 μstrain day^{-1}; 3 days	1^a
Serra Pizzuta – M. Stempato line	>0.550, 1.920 μstrain day^{-1}; 1 month	1^a
M. Siilvestri – Bocche 1792 line	>0.550, 1.920 μstrain day^{-1}; 1 month	1^a
Clinometric Variation (>5 μrad hour^{-1}; 3 stations)	=1; 1 day	1^a
SO_2 emission (>11000 ton day^{-1})	=1; 1 week	1^a
CO_2 emission (P78 station)	<50 g m^{-2} day^{-1}; 2 days	1^a
Gravity (E-W profile)	>4.30, 7.15 μGal day^{-1}; 15 days	1^a
Gravity (N-S profile; seasonal)	>5.70, 8.60 μGal day^{-1}; 15 days	1^a
NODE 4: Vent location		
Prior distribution	No info (uniform distribution)	
Past data (5 sectors, according topography; 1=summit area 2=eastern flank, 3=southern flank, 4=western flank, 5=northern flank)	y_4^1=118 y_4^2=13, y_4^3=8 y_4^4=2 y_4^5=12	

episodes with no eruption; this totals 31 unrest episodes spread over a period of 329 weeks (Table 1). The latter is calculated as the difference between the whole period (11 years, i.e., 574 weeks) and the total time (276 weeks) during which Mt. Etna was in unrest summed to the 31 total episodes.

3.1.2. Monitoring component

We considered 16 parameters. Relative order relations, thresholds, as well as inertia time windows are given in Table 1. Most of the parameters involved in the analysis are assumed as precursors when they show an increasing trend (i.e., increase of earthquake number and/or tremor amplitude for seismic activity, inflation for ground deformation, positive variation for relative gravity values). A large number of published papers supports the result of the elicitation process (Bonaccorso *et al*., 2002, 2004b; Alparone *et al*., 2003; Carbone *et al*., 2003; Patanè *et al*., 2003; Bonforte *et al*., 2004; Carbone and Greco, 2007; Falsaperla *et al*., 2005; among the most recent ones).

Conversely, the results of the elicitation for gases (both soil CO_2 and crater SO_2 emissions) need a more detailed explanation. The former, normally increases some months before the

occurrence of an eruption, as a result of exsolution from deep (>5 km) magma sources (Bruno *et al*., 2001; Aiuppa *et al*., 2004). The monitoring of CO_2 is performed by focusing on two areas, characterized by the highest gas concentration anomalies in soils, and located, respectively, in the central area of the eastern flank (P78 station, see Fig. 2), and on the lower SW flank of the volcano (P39 station, see Fig. 2). Both sites are known for being connected to deep faults that allow the escape of magmatic gases. P39 is inferred to drain gas from a deep magma source (>15 km), whereas P78 is related to a shallower reservoir [5-10 km; Bruno *et al*. (2001)]. Crater SO_2 emissions, conversely, are related to shallower (<4 km) magma dynamics. For both parameters, the volcano is considered in an unrest phase when an anomalous decreasing trend is observed (see Table 1), but relative meaning is different. In particular, CO_2 decreases following anomalous increases when magma moves rapidly towards shallower crustal levels at lower confining pressure. Therefore, large amounts of CO_2 exsolve from the melt into gas bubbles that rise up in the conduits either by buoyancy or carried by the moving magma, producing, then, a decreased flux of gases released into the enclosing rocks. The decrease in SO_2 flux is usually observed prior to an eruptive activity and might be related to periods of sealing of the magma body (Casadevall *et al*., 1981). Sometimes, it is possible to relate it to a deep seismic activity producing a depressurization of the system that draws the exsolved gas into relatively deep opening fractures, thus decreasing the emission from the summit craters (Caltabiano *et al*., 1994). The subsequent ascent of new magma is usually accompanied by a progressive rise in SO_2 flux starting from minimum relative values (Caltabiano *et al*., 1994).

The decreasing trend therefore, continues for CO_2 emissions before eruptions, whereas, SO_2 emissions show an inverted trend after a minimum is reached, then an increase starts, that may culminate in an eruption.

3.2. Node 2: magma / no magma

3.2.1. Non-monitoring component

A priori distribution. Given the detection of an unrest episode, we assume that it has a 95% probability of having a magmatic origin; this value is what is usually assumed worldwide for volcanoes such as Mt. Etna (C. Newhall personal communication), and it means that 95% of the unrest episodes are of magmatic origin. The number of equivalent data for this distribution is set to 1, thus, indicating large uncertainty.

Past data. There are no non-monitoring data that can be retrieved for this node.

3.2.2. Monitoring component

For this node, we chose 12 parameters (Table 1). The weight of each parameter is set to 1 by default, but when there is evidence of a particularly significant parameter, its weight is raised to 2. Thus, a weight of 2 is assumed for seismicity and gravity parameters. No past monitored events are present.

3.3. Node 3: eruption / no eruption

3.3.1. Non-monitoring component

A priori distribution. As for node 1, no information is available; again, a uniform distribution is assumed.

Past data. Considering the period January 1980 – December 1990, 17 unrest episodes out of 31 were marked by eruptions (see node 1).

3.3.2. Monitoring component

We chose 11 monitoring parameters (Table 1). As for node 2, a weight of 1 is assigned by default, whereas a weight of 2, again puts in evidence, the strong eruption forecasting capacity of seismic and gravimetric parameters (Table 1).

3.4. Node 4: location of the vent

3.4.1. Non-monitoring component

A priori distribution. We considered an a priori model for node 4 based on the present tectonic and volcanic structure of Mt. Etna, based in particular on past vent and fracture location data sets [eruptive history of the volcano during 20th century; Branca and Del Carlo (2005)]. We made this choice for homogeneity. Even if information on the flank volcanic activity has been quite reliable since the 18th century (Fig. 5), summit volcanic activity data are complete starting from 20th century, only (Branca and Del Carlo, 2005).

We provide a graphical frame (as each panel of Fig. 8), that takes into account the geography and the geometry of the volcano. The lower left corner is set at the point (northing 4,155,000 m, and easting 482,500 m, UTM zone 33), while the upper right corner at the point (northing 4,192,500 m, and easting 520,000 m). The centre of the frame is set in the summit crater area at the point (northing 4,178,110 m, and easting 499,505 m).

The investigated area is a circle, centred at the last defined point, with an inner circle and a surrounding annulus, in turn divided into four quadrants. The inner circle encloses the summit area and has a radius of 1 km; the annulus has an 11 km outer radius, and its quadrants are defined by radii trending NE-SW and NW-SE. Thus, quadrant 1 corresponds to the eastern flank, quadrant 2 to the southern one, quadrant 3 to the western one, and quadrant 4 to the northern one. The annulus comprises the area of the vents of the flank activity at Mt. Etna during 20th century (Branca and Del Carlo, 2005). Like nodes 1 and 3, a uniform distribution is assumed.

Past data. Following Branca and Del Carlo (2005), during 20th century Mt. Etna experienced 153 eruptive episodes, distinct due to their summit or flank vent sites, and distributed over the above zones (Fig. 5). Among these, 118 eruptive episodes involved the summit crater area, that has experienced the largest variety of eruptive activities (degassing, Strombolian phenomena, lava fountaining, lava emissions), whereas at lateral vents the activity is mostly related to lava flow emission. As in Marzocchi *et al*. (2008) the counts of past eruptive vents for each area (given in Table 1) are used to shape the likelihood function.

3.4.2. Monitoring component

No specific monitoring parameters are set for this node, but all the parameters set for preceding nodes could be suitable for assessing the future vent opening probability (Marzocchi *et al*., 2008).

In particular, we considered recorded seismic activities (both earthquakes and volcanic tremor) set in nodes 1, 2 and 3 as the most significant for the next vent opening because strongly localized.

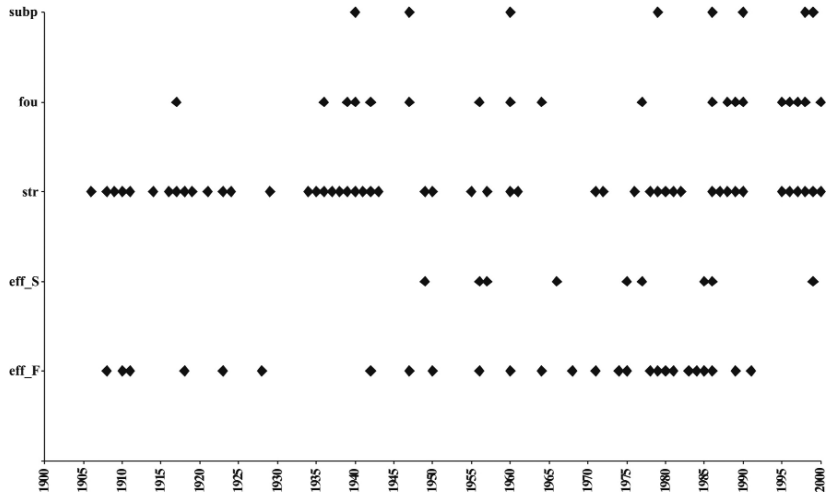

Fig. 5 - Occurrence of different style eruptions (subp=sub-Plinian, fou=lava fountains, str=Strombolian, eff_S=summit effusive, eff_F=flank effusive) at Mt. Etna during 20th century (see text for details).

3.5. Node 5: size / style of the initial phase of the eruption

For this node, the theoretical approach (i.e., Sandri *et al*., 2004) has proved, up to now that no monitoring parameter is able to provide insights into the size and style of an impending eruption. However, this could be possible at a well monitored and very active volcano such as Mt. Etna. Nevertheless, the elicitation of parameters able to discriminate among incoming Strombolian, fountains and sub-Plinian eruptions needs parameters whose quality was not available in 2001, as well as three-component, broadband seismometers, continuous GPS and gravimetric measurements, infrasound sensors, thermal cameras, etc. They are actually available at Mt. Etna; unfortunately they were not in 2001. Thus, node 5 will not be treated here.

4. Results of the 2001 eruption forecast

Concerning only a priori models and past data sets of the previous section, an average value in the long-term, absolute probability of eruption around 5.0% per week is retrieved (Fig. 6).

For the short-term eruption forecasting, the use of the monitoring component is needed. Therefore, by using monitoring parameters, we can estimate probabilities associated with significant variations of the volcanic phenomena over a time scale comparable to the fixed time window forecast (in our case, one week).

We focused our attention on the onset of the July - August 2001 eruption. Fig. 7b shows the chronology of the eruptive activities of Mt. Etna during the time interval January 1 - August 9 2001 (the end of the eruption). The BET_EF was applied over the time period January 1 - July 23 2001.

Starting from January up to July 9, we usually ran the process at a weekly rate. If "anomalous" data (i.e., monitoring parameters that exceed their thresholds) were observed, the model was run at a daily rate (e.g., April 20 – 21, May 7 –10). From July 12 up to July 23, we ran the process at a daily rate. In any case, the forecast time window remained fixed at one week. After this date,

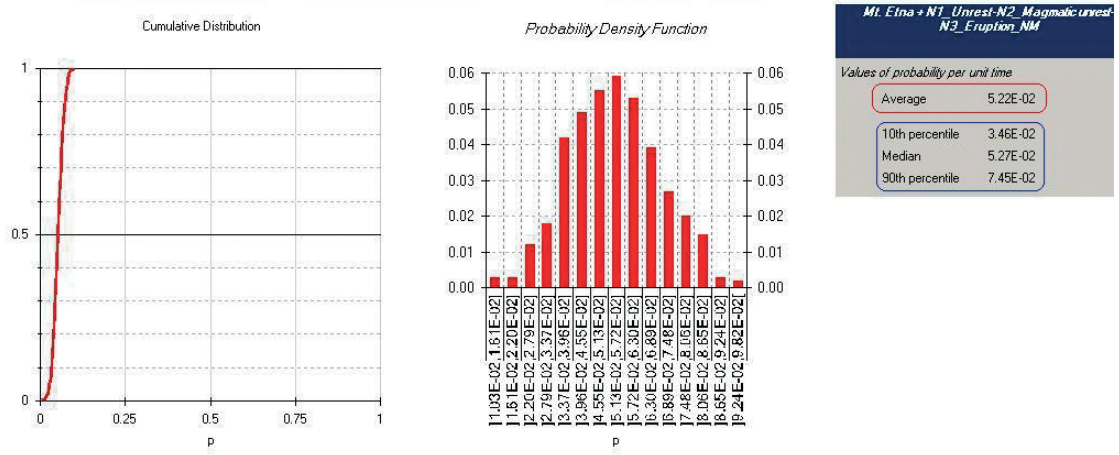

Fig. 6 - Graphical output of the BET_EF software package referred to the absolute probability estimate for node 3 (eruption node). The blue rectangular box encloses the median probability value calculated for the non-monitoring component; also shown the errors (10th and 90th percentile). Also given the average probability (red rectangular box).

monitoring parameters were recorded with coarser data.

Fig. 7a displays absolute probability estimates for node 1 as well as conditional probability values for node 2 and 3, respectively, and Table 2 summarizes all the above values.

At node 1, the absolute probability value of unrest is 100% for the whole time period (Fig. 7a, Table 2). This is due to the presence of at least one anomaly in the elicited parameters. In our case, they were both crater SO_2 and ash emissions, as well as clinometric data. This first result may seem obvious, being an active volcano as Mt. Etna almost always is in a state of unrest.

At node 2, the conditional probability of magmatic unrest is more than 93.0% for the whole time period (Fig. 7a, Table 2). This is obviously confirmed by the observed volcanic activity (Fig. 7b). Generally speaking, this confirms the very frequently observed involvement of magma during an unrest phase, whereas purely phreatic eruptions are rare (Branca and Del Carlo, 2005).

At node 3, the conditional probabilities of eruption are modulated by the presence of anomalies of monitoring parameters. The "background" (i.e., when no anomaly is observed) conditional probability of eruption is, on average, 28.0% (Fig. 7a, Table 2). If we translate this conditional 28.0% into an absolute probability of eruption (multiplying it by the conditional probability of magma and by the probability of unrest), we obtain 26.8% (on average). This "background" value was almost constant until April 20, 2001, when a sharp increase in the probability of eruption (83.6%) occurred (Fig. 7a). This is only due to an earthquake swarm occurring on the volcano (recall that the inertia time for seismic activity is 1 day for node 3; Table 1). On the following day, the probability estimate suddenly dropped to the "background" level. The probability estimates flattened to the "background" level until early May 2001, when high probability values (68.0% and 82.1%, on May 7 and 9, respectively; Fig. 7a, Table 2), due to monitoring anomalies in tremor data was estimated. In fact, a short lived (a few hours) lava fountain eruption occurred on May 9 (Fig. 7b).

Later, a high probability increasing level starting from June 2 up to early July (on average,

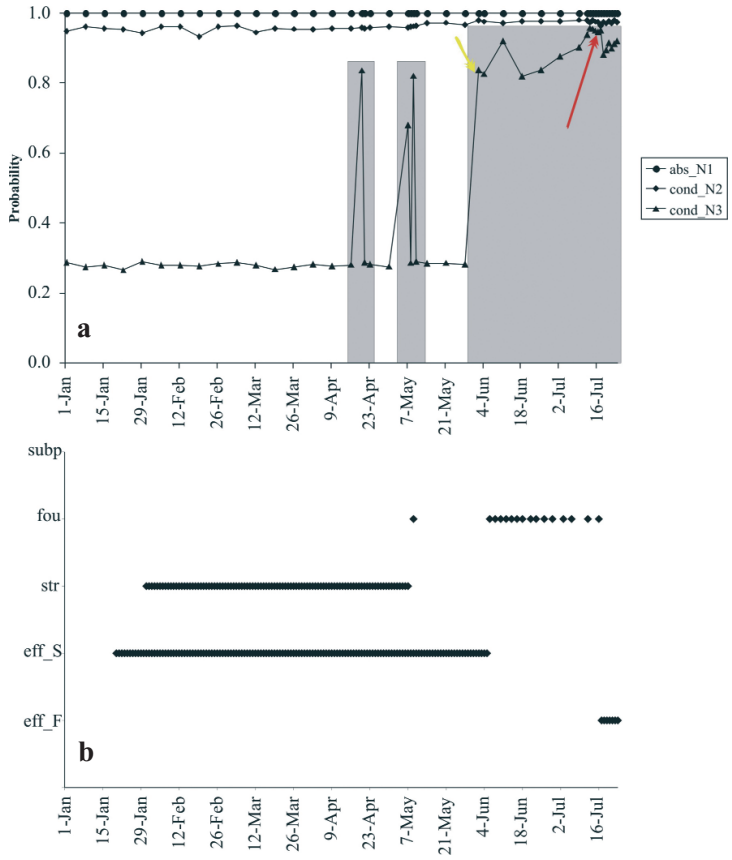

Fig. 7 - (a.) Probability estimations during the 2001 January 1-July 23 time period at Mt. Etna. Different symbols display different estimates: circles stand for absolute probability for node 1 (unrest), diamonds stand for conditional probability for node 2 (magmatic unrest, given an unrest), and triangles stand for conditional probability for node 3 (eruption, given a magmatic unrest). Gray boxes put in evidence periods of anomalous signals in the monitored parameters producing high probability estimates. Yellow arrow indicates the onset of the June 7-July 16 lava fountaining at SEC and red arrow indicates the July 17-August 9 flank eruption activity. (b.) Eruption styles vs. time, during January 1-July 23 [data from Behncke *et al.* (2006)]. The y-axis as in Fig. 5.

more than 85.0%) was observed (Fig. 7a). During the same time period 13 lava fountain eruptions occurred at SEC (Fig. 7b), as well as the lava effusion from the fissure at the base of SEC was still ongoing (Behncke *et al.*, 2006).

Starting from July 9 up to 23, the mean probability estimates were, on average, 92.5%, with a maximum peak that occurred on July 13 (95.8%; Fig. 7a, Table 2), the starting day of the VT seismicity that preceded the lava emission until July 18 (Patanè *et al.*, 2003). On July 17, the day of the flank eruption onset, the probability estimate reached a value of 95.2% (Fig. 7a, Table 2).

Concerning node 4 (vent location), VT earthquakes (depth < 5 km) and volcanic tremors are the most significant anomalous parameters in the investigated period. Thus, by considering both, we generated maps showing relative probabilities of vent opening in the different zones, for early May and middle July 2001 (Fig. 8). The eventual vent site fell consistently within the highest probability zone on all of the maps (Fig. 8). Table 3, reports the absolute probability values spread over the different sectors of the graphical frame defined above only for the days in which the probability of eruption (node 3) rose up over 60% (Fig. 7a, Table 2). In May, a higher probability is observed in the summit crater zone (Fig. 7a). Indeed, the activity at SEC extended from early May up to the middle of July, as described above (Fig. 7b).

Starting from July 12, the probability of eruptive activity, mostly effusive, became present in

the southern quadrant, too. Starting from July 16 (Fig. 8) there is a strong increases there. Indeed, the first flank eruptive system opened on July 17 from 2900 to 2700 m a.s.l., while the lower eruptive fracture (2100 m a.s.l.) opened on July 18 (Monaco *et al*., 2005).

5. Final remarks

A recently-developed technique for probabilistic forecasting (BET_EF) has been applied to quiescent volcanoes [e.g., Vesuvius; Marzocchi *et al*. (2004, 2008)] or calderas [e.g., Campi Flegrei, Orsi *et al*. (2009) and Auckland Volcanic Field, Lindsay *et al*. (2010)] with different elicitation experiments.

Before this application was used, it was unclear how the code might work on a persistently active, open conduit volcano, such as Mt. Etna. The historical eruptive catalogue, coupled with the modern monitoring records available makes it a reliable laboratory for testing the procedure. Our preliminary results suggest that the BET_EF can be applied to such kinds of volcanoes.

A very important aspect of this application was the monitoring setting experiment. An improved workflow that created a direct interface between qualitative, process-based knowledge, and quantitative information is therefore significantly useful. For Mt. Etna, the adopted code manages a relevant set of past data and a priori models set by the end user, as well as monitoring data that must be gained by an advisory group of experts usually before a crisis. This code then has a huge potential for optimizing and clarifying decision-making procedures. In the light of this view, the technique will rapidly translate (in near real time) our subjective decisions into objective probabilities as information about unrest evolves, and may be used as a rational starting point for further discussions.

We focused our attention for the "well predictable" eruption as the one that occurred in 2001 at Mt. Etna, the first case-history of an activity monitored with a good-quality multidisciplinary monitoring system. Our estimated calculations seem suitable for managing eruptive crises with a sufficient alert time, since they clearly showed an increase in the eruption probability at least one month before the eruption onset (Fig. 7a), as well as the fact that the space-time evolution of the eruptive scenario was roughly predicted (Fig. 8).

The monitoring parameters were set taking into account the present state of the surveillance system, and relative thresholds and inertia time window were fixed looking at the recent evolution of the relative time series.

Therefore, the present application shows that the monitoring had a primary role, because the estimated probabilities are able to trace the time evolution of the state of the volcano coherent with what really occurred.

The strong evidence is based on the probability values of the unrest (node 1). The 100% estimate for the whole period (2001 January 1-July 23; Fig. 7a) indicates that Mt. Etna is almost always under unrest, as expected for an active open-conduit volcano. The probability values higher than 93.0% for node 2 (magma/no magma; Fig. 7a) suggest that magma was strongly involved during the 2001 unrest phase studied here. Concerning node 3 (eruption/no eruption), the probability values yield to fix a "background" level (28.0% on average; Fig. 7a) when no monitoring anomalies are observed. In addition, when probabilities are estimated with values higher than 80.0% (Fig. 7a) an eruptive activity is incoming. Therefore, the value of 80.0% could

Table 2 - Average probability values as estimated for node 1 (absolute estimates), 2 (conditional estimates) and 3 (conditional estimates). Values referred to node 1 (unrest/no unrest) are equal to 100% because of the presence of at least an anomalous parameter, by definition (see text for details).

Date	**Node 1**	**Node 2**		**Node 3**	
	Absolute	Absolute	Conditional	Absolute	Conditional
2001/01/01	100%	95.6%	94.9%	28.3%	28.6%
2001/01/08	100%	95.9%	96.1%	28.1%	27.3%
2001/01/15	100%	94.6%	95.7%	27.4%	27.8%
2001/01/22	100%	96.7%	95.4%	26.3%	26.5%
2001/01/29	100%	96.9%	94.4%	27.0%	29.0%
2001/02/05	100%	95.8%	96.2%	27.7%	27.9%
2001/02/12	100%	94.6%	96.2%	25.9%	27.9%
2001/02/19	100%	96.0%	93.4%	25.6%	27.7%
2001/02/26	100%	93.7%	96.1%	26.7%	28.3%
2001/03/05	100%	94.9%	96.5%	27.0%	28.6%
2001/03/12	100%	96.9%	94.5%	26.1%	27.9%
2001/03/19	100%	96.9%	95.7%	26.9%	26.7%
2001/03/26	100%	94.5%	95.5%	26.7%	27.3%
2001/04/02	100%	95.6%	95.4%	26.7%	28.2%
2001/04/09	100%	95.5%	95.6%	27.7%	27.6%
2001/04/16	100%	95.8%	95.7%	25.8%	28.0%
2001/04/20	100%	94.0%	95.9%	77.8%	83.6%
2001/04/21	100%	95.6%	95.6%	25.3%	28.7%
2001/04/23	100%	96.2%	95.9%	27.0%	28.1%
2001/04/30	100%	96.2%	96.1%	26.9%	27.5%
2001/05/07	100%	97.2%	96.0%	66.1%	68.0%
2001/05/08	100%	96.1%	96.1%	26.1%	28.5%
2001/05/09	100%	97.5%	96.3%	81.1%	82.1%
2001/05/10	100%	96.7%	96.5%	27.7%	29.0%
2001/05/14	100%	97.4%	97.2%	26.7%	28.4%
2001/05/21	100%	96.7%	97.3%	27.8%	28.5%
2001/05/28	100%	96.9%	96.7%	27.6%	28.2%
2001/06/02	100%	96.6%	97.9%	80.6%	83.7%
2001/06/04	100%	97.7%	97.6%	80.4%	82.6%
2001/06/11	100%	97.2%	97.2%	89.1%	92.0%
2001/06/18	100%	97.8%	97.7%	80.7%	82.0%
2001/06/25	100%	97.6%	97.8%	80.7%	83.7%
2001/07/02	100%	97.5%	97.7%	86.7%	87.7%
2001/07/09	100%	98.2%	98.1%	88.4%	90.2%
2001/07/12	100%	96.7%	97.9%	93.7%	93.9%
2001/07/13	100%	96.6%	97.3%	94.9%	95.8%
2001/07/14	100%	97.3%	97.9%	91.4%	95.5%
2001/07/15	100%	97.7%	97.6%	92.8%	95.0%
2001/07/16	100%	97.8%	97.5%	92.5%	94.7%
2001/07/17	100%	98.1%	96.4%	91.8%	95.2%
2001/07/18	100%	97.5%	97.5%	86.4%	88.1%
2001/07/19	100%	96.7%	97.1%	87.7%	89.4%
2001/07/20	100%	97.4%	97.7%	88.9%	91.5%
2001/07/21	100%	97.2%	97.1%	88.4%	89.8%
2001/07/22	100%	97.2%	97.9%	88.2%	91.3%
2001/07/23	100%	97.9%	97.4%	86.7%	92.0%

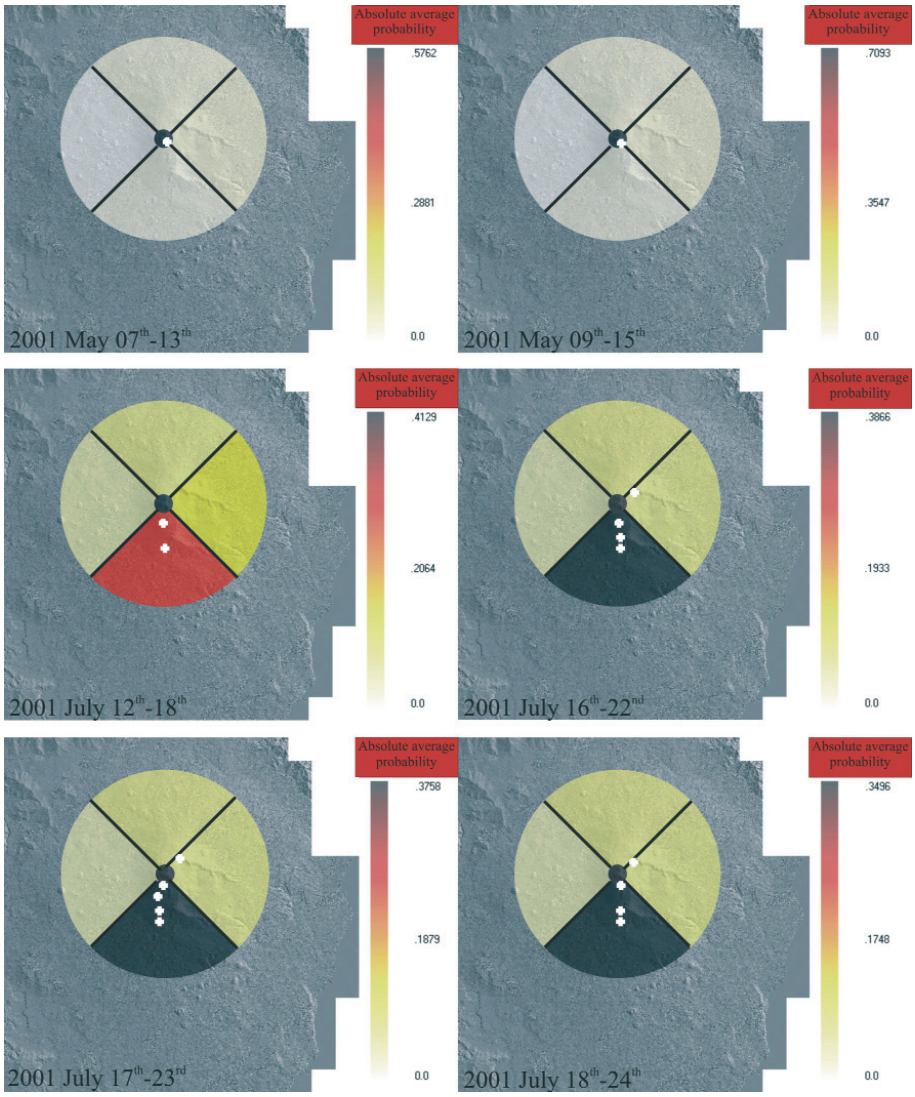

Fig. 8 - Maps showing the space-time probability of eruptive vent opening on some selected periods. The colour scale bar at right of each panel represents the average absolute probability as spread over the graphical sectors considered in this study. Thick lines separate the flank sectors (see text for details). Also shown (white crosses) the location of the eruptive vents that opened during the related one week probability window (see Fig. 3 for comparison).

be arbitrarily chosen as a first alert threshold. Finally, for node 4, the predicted vent location (Fig. 8) seems to match the eruptive scenario that actually occured.

Some final remarks must be made. Indeed, some features might be more adapted to the Mt. Etna volcano for future applications. The large number of parameters, if compared with those elicited in other theoretical cases (e.g., Vesuvius, Campi Flegrei, Auckland Volcanic Fields), and used for defining the different nodes seem to be barely applicable in a real-case scenario. Due to the present code setting, the most relevant strategy is based on do not neglect any of the most informative monitored parameters. This assures us that, during a crisis, we are able to estimate

Table 3 - Average absolute probabilities estimated for node 4 (vent locations). Reported values are referred to those days in which probability of eruption rose to over 60.0% (node 3 in Table 2).

Date	Node 4				
	Summit area	Eastern flank	Southern flank	Western flank	Northern flank
2001/04/20	33.7%	11.4%	26.0%	2.7%	5.2%
2001/05/07	57.6%	2.9%	1.9%	0.6%	2.7%
2001/05/09	70.9%	3.6%	2.3%	0.8%	3.3%
2001/06/02	60.8%	7.2%	4.6%	1.5%	6.6%
2001/06/04	60.3%	7.1%	4.6%	1.5%	6.6%
2001/06/11	66.3%	7.8%	5.0%	1.7%	7.3%
2001/06/18	59.7%	7.0%	4.5%	1.5%	6.5%
2001/06/25	59.1%	7.0%	4.5%	1.5%	6.5%
2001/07/02	64.1%	7.5%	4.9%	1.6%	7.0%
2001/07/09	66.5%	7.8%	5.0%	1.7%	7.3%
2001/07/12	41.3%	13.3%	26.3%	4.2%	7.1%
2001/07/13	37.3%	6.7%	38.2%	3.5%	6.4%
2001/07/14	36.4%	6.6%	37.2%	3.4%	6.3%
2001/07/16	37.8%	6.8%	38.7%	3.6%	6.5%
2001/07/17	36.8%	6.6%	37.6%	3.5%	6.3%
2001/07/18	34.2%	6.2%	35.0%	3.2%	5.9%
2001/07/19	35.3%	6.6%	34.4%	3.6%	6.4%
2001/07/20	35.8%	7.1%	32.7%	4.1%	6.8%
2001/07/21	36.6%	7.2%	33.4%	4.2%	7.0%
2001/07/23	36.7%	7.3%	33.5%	4.2%	7.0%

probabilities even if some anomalous measures are missing. In any case, an anomalous parameter is not suitable to assess a heralding eruptive activity, as shown for the “false alarm” on April 20, when a suddenly anomalous increase in shallow earthquakes occurred.

The adopted boxcar-shaped, inertia time window may lead to some spurious results. A suitable alternative would be to use time-weighted inertia windows, by considering for instance that the weight of a given parameter decreases exponentially with time after it first exceeds the defined threshold. Further applications can test if this suggestion can be meaningful or not, as well as new weight assignment which could better explain the role of the most significant monitoring parameters.

A different vent location geometry (e.g., squared cells) is more appropriate if looking at the distribution of the flank activity that can evolve with the opening of more than one single eruptive fracture on the slopes of the volcano.

Additionally, the proposal of a reliable statistical model of the historical eruptive activity at Mt. Etna could be taken into account in order to better combine the size and the type of eruption.

As Mt. Etna experienced a wide variety of eruptive activities, establishing the BET_EF code

for this volcano will address a scientific discussion on how a future eruption might progress.

In conclusion, our results stressed the potential of the BET_EF procedure, through the quality of the monitoring input data set, thus providing a rational means for their revision when new data or information are incoming.

Acknowledgments. The authors wish to thank Chris Newhall for the fruitful discussions and suggestions. The constructive criticism of two anonymous reviewers has been greatly appreciated. The authors, also, wish to thank Dario Albarello and Carlo Meletti for their kind invitation in submitting this paper. The present paper follows an oral contribution at the XXVIII Annual GNGTS Meeting (16-19 November 2009, Trieste, Italy). This research has benefited from funding provided by the Italian Presidenza del Consiglio dei Ministri - Dipartimento della Protezione Civile (DPC, 2007-2009-10 V3 'Lava' project). Scientific papers funded by DPC do not represent any official opinion or policies.

REFERENCES

Aiuppa A., Allard P., D'Alessandro W., Giammanco S., Parello F. and Valenza M.; 2004: *Magmatic gas leakage at Mount Etna (Sicily, Italy): relationships with the volcano-tectonic structures, the hydrological pattern and the eruptive activity.* In: Bonaccorso A., Calvari S., Coltelli M., Del Negro C. and Falsaperla S. (eds), Mt. Etna: Volcano Laboratory. American Geophysical Union, Washington DC, pp. 129-145, doi.: 10.1029/143GM09.

Alparone S., Andronico D., Lodato L. and Sgroi T.; 2003: *Relationship between tremor and volcanic activity during the Southeast Crater eruption on Mount Etna in early 2000.* J. Geophys. Res., **108** (B5), doi: 10.1029/2002JB001866.

Behncke B., Neri M., Pecora E. and Zanon V.; 2006: *The exceptional activity and growth of the Southeast Crater, Mount Etna (Italy), between 1996 and 2001.* Bull. Volcanol., **69**, 149-173, doi: 10.1007/s00445-006-0061-x.

Bonaccorso A., Aloisi M. and Mattia M.; 2002: *Dike emplacement forerunning the Etna July 2001 eruption modelled through continuous tilt and GPS data.* Geophys. Res. Let., **29** (13), doi: 10.10129/2001GL014397.

Bonaccorso A., Calvari S., Coltelli M., Del Negro C. and Falsaperla S. (eds); 2004a: *Mt. Etna: Volcano Laboratory.* American Geophysical Union, Washington DC, 357 pp.

Bonaccorso A., D'Amico S., Mattia M. and Patanè D.; 2004b: *Intrusive mechanism at Mt. Etna forerunning the July-August 2001 eruption*. Pure Appl. Geophys., **161**, doi: 10.1007/s00024-004-2515-4.

Bonforte A., Guglielmino F., Palano M. and Puglisi G.; 2004: *A syn-eruptive round deformation episode measured by GPS, during the 2001 eruption on the upper southern flank of Mt. Etna.* Bull. Volcanol., **66**, 336-341, doi: 10.1007/s0045-003-0314-x.

Branca S. and Del Carlo P.; 2005: *Types of eruptions at Etna volcano AD 1670-2003: implications for short-term eruptive behaviour.* Bull. Volcanol., **67**, 737-742 doi: 10.1007/s00445-005-0412-z.

Bruno N., Caltabiano T., Giammanco S. and Romano R.; 2001: *Degassing of SO2 and CO2 at Mount Etna (Sicily) as an indicator of pre-eruptive ascent and shallow emplacement of magma.* J. Volcanol. Geotherm. Res., **110**, 137-153.

Caltabiano T., Romano R. and Budetta G.; 1994: *SO_2 flux measurements at Mount Etna (Sicily).* J. Geophys. Res., **99** (D6), 12809-12819.

Carbone D. and Greco F.; 2007: *Review of microgravity observations at Mt. Etna: a powerful tool to monitor and study active volcanoes.* Pure Appl. Geophys., **164**, 769-790, doi: 10.1007/s00024-007-0194-7.

Carbone D., Budetta G. and Greco F.; 2003: *Bulk processes prior to the 2001 Mount Etna eruption, highlighted through microgravity studies.* J. Geophys. Res., **108**, doi: 10.1029/2003JB002542.

Casadevall T.J., Johnston D.A., Harris D.M., Rose W.I., Malinconico L.L., Stoiber R.E., Bornhorst T.J., Williams S.N., Woodruff L. and Thompson J.M.; 1981: *SO_2 emission rates at Mount St. Helens from March 29 through December, 1980.* In: Lipman P.W. and Mullineaux D.R. (eds), The 1980 eruptions of Mount St. Helens, U. S. Geol. Surv. Prof. Pap. 1250, pp. 193-200.

Cocina O., Neri G., Privitera E. and Spampinato S.; 1998: *Seismogenetic stress field beneath Mt. Etna (South Italy) and possible relationship with volcano-tectonic features*. J. Volcanol. Geotherm. Res., **83**, 335-348.

Cristofolini R., Gresta S., Imposa S. and Patanè G.; 1988: *Feeding mechanism of eruptive activity at Mt. Etna based on seismological and petrological data.* In: King L.Y. and Scarpa R. (eds), Modeling of Volcanic Processes. Earth Evol. Sci, pp. 73-93.

Falsaperla S., Alparone S., D'Amico S., Di Grazia G., Ferrari F., Langer H., Sgroi T. and Spampinato S.; 2005: *Volcanic tremor at Mt. Etna, Italy, preceding and accompanying the eruption of July-August 2001.* Pure and App. Geophys., **162**, 2111-2132, doi: 10.1007/s00024-005-2710-y.

Guest J.E.; 1982: Styles of eruptions and flow morphology on Mt. Etna (volcanological data). Mem. Soc. Geol. It., **23**, 49-73.

Lindsay J., Marzocchi W., Jolly G., Costantinescu R., Selva J. and Sandri L.; 2010: *Towards real-time eruption forecasting in the Auckland Volcanic Field: application of BET_EF during the New Zealand National Disaster Exercise 'Ruamoko'.* Bull. Volcanol., **72**, 185-204, doi: 10.1007/s00445-009-0311-9.

Marzocchi W., Sandri L., Gasparini P., Newhall C. and Boschi E.; 2004: *Quantifying probabilities of volcanic events: the example of volcanic hazard at Mount Vesuvius.* J. Geophys. Res., **109**, B11201, doi: 10.1029/2004JB00315U.

Marzocchi W., Sandri, L. and Selva, J.; 2008: *BET_EF: a probabilistic tool for long- and short-term eruption forecasting.* Bull. Volcanol., **70,** 623-632, doi: 1007/s00445-007-0157-y, 2008.

Monaco C., Catalano S., Cocina O., De Guidi G., Ferlito C., Gresta S., Musumeci C. and Tortorici L.; 2005: *Tectonic control on the eruptive dynamics at Mt. Etna volcano (Sicily) during the 2001 and 2002-2003 eruptions*. J. Volcanol. Geotherm. Res., **144**, 211-233, doi: 10.1016/j.jvolgeores.2004.11.024.

Newhall C.G. and Hoblitt R.P.; 2002: *Constructing event trees for volcanic crises.* Bull. Volcanol., **64**, 3-20 doi: 10.1007/s004450100173.

Orsi G., Di Vito M.A., Selva J. and Marzocchi W.; 2009: *Long-term forecast of eruption style and size at Campi Flegrei caldera (Italy).* Earth Planet. Sci. Let., **287,** doi: 10.1016/j.epsl.2009.08.013.

Patanè D., Privitera E., Gresta S., Akinci A., Alparone S., Barberi G., Chiaraluce L., Cocina O., D'Amico S., De Gori P., Di Grazia G., Falsaperla S., Ferrari F., Gambino S., Giampiccolo E., Langer H., Maiolino V., Moretti M., Mostaccio A., Musumeci C., Piccinini D., Reitano D., Scarfì L., Spampinato S., Ursino A. and Zuccarello L.; 2003: *Seismological constraints for the dike emplacement of July-August 2001 lateral eruption at Mt. Etna volcano, Italy.* Ann. Geophys., **46**, 599-608.

Sandri L., Marzocchi W. and Zaccarelli L.; 2004: *A new perspective in identifying the precursory patterns of volcanic eruptions.* Bull. Volcanol., **66**, 263-275, doi: 10.1001/s00445-003-0309-7.

Corresponding author: Alfonso Brancato
Dipartimento di Scienze Geologiche, Università degli Studi di Catania
Corso Italia 55, 95129 Catania
Phone: +39 095 7195709; fax: +39 095 7195728; e-mail: abranca@unict.it